


RESEARCH ARTICLE

Open Access



Dynamic predictive accuracy of electrocardiographic biomarkers of sudden cardiac death within a survival framework: the Atherosclerosis Risk in Communities (ARIC) study

Erick A. Perez-Alday^{1,2}, Aron Bender^{1,3}, David German¹, Srinivasa V. Mukundan^{1,4}, Christopher Hamilton^{1,5}, Jason A. Thomas^{1,6}, Yin Li-Pershing¹ and Larisa G. Tereshchenko^{1,7*} 

Abstract

Background: The risk of sudden cardiac death (SCD) is known to be dynamic. However, the accuracy of a dynamic SCD prediction is unknown. We aimed to measure the dynamic predictive accuracy of ECG biomarkers of SCD and competing non-sudden cardiac death (non-SCD).

Methods: Atherosclerosis Risk In Community study participants with analyzable ECGs in sinus rhythm were included ($n = 15,716$; 55% female, 73% white, age 54.2 ± 5.8 y). ECGs of 5 follow-up visits were analyzed. Global electrical heterogeneity and traditional ECG metrics (heart rate, QRS, QTc) were measured. Adjudicated SCD was the primary outcome; non-SCD was the competing outcome. Time-dependent area under the receiver operating characteristic curve (ROC(t) AUC) analysis was performed to assess the prediction accuracy of a continuous biomarker in a period of 3,6,9 months, and 1,2,3,5,10, and 15 years using a survival analysis framework. Reclassification improvement as compared to clinical risk factors (age, sex, race, diabetes, hypertension, coronary heart disease, stroke) was measured.

Results: Over a median 24.4 y follow-up, there were 577 SCDs (incidence 1.76 (95%CI 1.63–1.91)/1000 person-years), and 829 non-SCDs [2.55 (95%CI 2.37–2.71)]. No ECG biomarkers predicted SCD within 3 months after ECG recording. Within 6 months, spatial ventricular gradient (SVG) elevation predicted SCD (AUC 0.706; 95%CI 0.526–0.886), but not a non-SCD (AUC 0.527; 95%CI 0.303–0.75). SVG elevation more accurately predicted SCD if the ECG was recorded 6 months before SCD (AUC 0.706; 95%CI 0.526–0.886) than 2 years before SCD (AUC 0.608; 95%CI 0.515–0.701). Within the first 3 months after ECG recording, only SVG azimuth improved reclassification of the risk beyond clinical risk factors: 18% of SCD events were reclassified from low or intermediate risk to a high-risk category. QRS-T angle was the strongest long-term predictor of SCD (AUC 0.710; 95%CI 0.668–0.753 for ECG recorded within 10 years before SCD).

(Continued on next page)

* Correspondence: tereshch@ohsu.edu

¹Knight Cardiovascular Institute, Department of Medicine, Oregon Health & Science University School of Medicine, 3181 SW Sam Jackson Park Rd; UHN62, Portland, OR 97239, USA

⁷Cardiovascular Division, Department of Medicine, Johns Hopkins University School of Medicine, Baltimore, MD, USA

Full list of author information is available at the end of the article



(Continued from previous page)

Conclusion: Short-term and long-term predictive accuracy of ECG biomarkers of SCD differed, reflecting differences in transient vs. persistent SCD substrates. The dynamic predictive accuracy of ECG biomarkers should be considered for competing SCD risk scores. The distinction between markers predicting short-term and long-term events may represent the difference between markers heralding SCD (triggers or transient substrates) versus markers identifying persistent substrate.

Keywords: Electrocardiography, Sudden cardiac death, Vectorcardiography, Dynamic prediction, Global electrical heterogeneity

Background

Sudden cardiac death (SCD) is a major contributor to cardiovascular mortality, accounting for 40–50% of the years of potential life lost from all cardiovascular diseases (CVD) [1, 2]. In the United States (US), more than 350,000 emergency medical services-assessed out-of-hospital sudden cardiac arrests occur annually [1]. There remains a lack of reliable, dynamic predictors of SCD [3]. An electrocardiogram (ECG) can characterize the presence and properties of the electrophysiological substrate of SCD. Our group recently showed that global electrical heterogeneity (GEH), as measured by five metrics [spatial QRS-T angle, spatial ventricular gradient (SVG) azimuth, elevation, and magnitude, and sum absolute QRST integral (SAI QRST)] is independently (after comprehensive adjustment for time-updated CVD events and their risk factors) associated with SCD, representing an underlying substrate of SCD [4]. The subsequent discovery of 10 genetic loci, associated with GEH at a genome-wide significance level, confirmed the presence of several underlying mechanisms behind the GEH ECG phenotype [5]. We also developed a competing risk score of SCD and showed that the addition of GEH measures to clinical risk factors significantly improves the reclassification of SCD risk [4]. The risk of SCD is known to be dynamic. However, current risk models predict SCD using baseline risk factors measured at a single point in time. Therefore, evaluating the accuracy of a dynamic prediction is, therefore, necessary to better understand the temporal relationship between substrate and events. The goal of this study was to investigate the dynamic predictive accuracy of GEH and traditional ECG biomarkers of SCD within a survival framework in comparison with competing non-sudden cardiac death (non-SCD) in the Atherosclerosis Risk in Community (ARIC) study participants.

Methods

Study population

The ARIC study is an ongoing prospective cohort study evaluating risk factors, progression, and outcomes of atherosclerosis in 15,792 participants (45% male, 74% white) enrolled in four US communities in 1987–1989. The ARIC study protocol and design have been

previously described [6]. We excluded ARIC participants with absent or poor-quality ECGs due to noise, artifacts, or missing leads ($n = 24$), atrial fibrillation (AF) ($n = 36$), and ventricular pacing ($n = 16$) at the baseline study visit. Only participants in normal sinus rhythm were included in this study ($n = 15,716$). If AF or ventricular pacing were diagnosed at any time during follow-up, such participants were included for a period until AF or ventricular pacing were diagnosed on 12-lead ECG. Prevalent CVD was defined as the presence of at least one baseline prevalent condition: coronary heart disease (CHD), heart failure (HF), stroke, peripheral artery disease (PAD), atrioventricular (AV) block II-III, atrial or ventricular pacing, or Wolff-Parkinson-White ECG phenotype.

Clinical characteristics of participants

Prevalent CHD was defined as a history of myocardial infarction (MI), or coronary revascularization via coronary artery bypass surgery or percutaneous coronary intervention. Prevalent MI was defined as a self-reported history of MI and/or ECG evidence of MI as defined by the Minnesota code [7]. Prevalent AF was defined as either a self-reported and validated history of AF or a diagnosis of AF on the baseline ECG. Prevalent HF was defined as self-reported use of HF medication or evidence of symptomatic HF as defined by stage 3 of the Gothenburg criteria [8], which required the presence of specific cardiac and pulmonary symptoms in addition to medical treatment of HF. Prevalent stroke in ARIC was defined by a stroke and transient ischemic attack diagnostic algorithm, as previously described [9]. PAD was defined as the ankle-brachial index ≤ 0.90 . Details of ankle-brachial index measurement in the ARIC study have been previously described [10].

Definition of a primary outcome: sudden cardiac death

A follow-up of ARIC participants was previously reported [11]. SCD was defined as a sudden pulseless condition in a previously stable individual without evidence of a non-cardiac cause of cardiac arrest if the cardiac arrest occurred out of the hospital or in the emergency room. To identify cases of SCD in ARIC, cases of fatal CHD that occurred by December 31, 2012 were reviewed and adjudicated by a committee of physicians

in two phases, as previously described [12]. CHD deaths occurring on or before December 31, 2001 were adjudicated in the first phase. CHD deaths occurring between January 1, 2002 and December 31, 2012 were adjudicated in the second phase. Available data from death certificates, informant interviews, physician questionnaires, coroner reports, prior medical history, and hospital discharge summaries were reviewed, in addition to circumstances surrounding the event. Each event was adjudicated independently by two physicians. In cases of disagreement, a third reviewer independently reviewed the event to provide final classification. Definite, probable, or possible SCD was included in this study as a primary outcome: the strength of available evidence determined this stratification. Definite SCD included cases of witnessed SCD with definite evidence such as an available rhythm strip of life-threatening cardiac arrhythmia, or primary emergency medical services impression of cardiac arrest. Probable SCD was defined as SCD with uncertainty either due to concomitant clinical conditions that can muddle the exact cause of demise, or limited information to adjudicate an event. Possible SCDs were adjudicated only in the second phase of reviews. The strength of evidence for probable SCD was greater than the strength of evidence for possible SCD. Possible SCD included cases of death that were unwitnessed but had specified SCD on a death certificate and did not document another cause of death. Participants were censored at the time of loss to follow-up, incident AF or ventricular pacing on 12-lead ECG, or death if the cause of death was any other than SCD.

Competing mortality outcome: non-sudden cardiac death

Cases of fatal CHD were adjudicated by the ARIC Morbidity and Mortality Classification Committee, as previously described [11]. Fatal CHD that did not meet the criteria of SCD comprised the non-SCD outcome.

12 lead ECG recording

12-lead ECG was recorded according to the ARIC study protocol and manual (version 1.0; August 1987). The method and procedure for 12-lead ECG recording, as described in the ARIC manual, are outlined below. During the baseline examination, a standard supine 12-lead ECG was recorded after a 12-h fast followed by a light snack and at least 1 h after smoking or ingestion of caffeine. The standard electrocardiograph for the ARIC study was the MAC PC by Marquette Electronics, Inc. A 12-lead resting ECG was obtained consisting of 10 s of each of the leads (I, II, III, aVR, aVL, aVF, V1-V6) simultaneously recorded. In an effort to enable longitudinal comparisons of ECGs, ARIC investigators developed and implemented a uniform procedure for electrode placement and skin preparation. The participant, stripped to

the waist, was instructed to lie on the recording bed with arms relaxed at the sides. The individual was asked to avoid movements that may cause errors in marking the electrode locations. For optimal electrode/skin interface, the electrodes were placed on the skin at least 2–3 min before recording the ECG. A pen was used to mark the six chest electrode positions. The chest was wiped with a sterile alcohol prep. Left leg electrode was placed on the medial surface of the left ankle. Right leg electrode was placed on the medial surface of the right ankle. Left arm electrode was placed on the medial surface of the left wrist. Right arm electrode was placed on the medial surface of the right wrist. Electrode V1 was located in the 4th intercostal space at the right sternal border, immediately to the right of the sternum. Electrode V2 was located in the 4th intercostal space, immediately to the left of the sternal border. Next, E-point was located by finding the 5th intercostal space, and following it horizontally to the midsternal line. Location of V6 electrode was found using the chest square. V6 was located at the same level as the E point in the midaxillary line (straight down from the center of the armpit). If breast tissue was over the V6 area, V6 was placed on top of the breast. No attempt was made to move the breast. Electrode V4 was located using a flexible ruler, as a midway between E and V6. Electrode V3 was located using a flexible ruler, midway between V2 and V4. Using a flexible ruler, electrode V5 was located midway between the locations of V4 and V6. After placing the electrodes on the skin, the participant's information was input to the MAC PC. It was required that electrodes must be on the skin for at least 3 min before taking the ECG. During the ECG recording, special attention was paid to the quality of recording. Quality control and technical troubleshooting procedures were in place to minimize errors (lead switch), noise, and artifacts. Recorded 12-lead ECGs were originally saved in the memory of the ECG machine and transmitted to a MUSE database (GE Marquette, Milwaukee, WI) within the Halifax ECG Computing Center via the phone line. Later, the MUSE database was transferred from the Halifax ECG Computing Center to the Epidemiological Cardiology Research Center (EPICARE, Wake Forest University, NC), and then to the Tereshchenko laboratory at Oregon Health & Science University.

Electrocardiogram analyses

ECG data from all five follow-up visits were analyzed. Traditional ECG intervals were reported by the 12 SL algorithm using Magellan ECG Research Workstation V2 (GE Marquette Electronics, Milwaukee, WI). QT interval was corrected for heart rate according to Bazett's formula. We analyzed raw, digital, 10-s, 12-lead ECGs (sampling rate of 500 Hz and amplitude resolution of 1 μ V).

Origin and conduction path of each cardiac beat was adjudicated by the team of physicians (DG, AB, SVM, LGT), and each beat was manually labeled by investigators (CH, JAT) for subsequent automated analyses. A representative normal sinus median beat was constructed. For the development of a normal sinus median beat, sinus beats before and after premature ventricular complexes, and noisy or distorted beats were excluded. In this study, only the normal sinus median beat was used for our analysis. GEH was measured as previously described, [4, 13] in a time-coherent median beat with the identified origin of the heart vector [14]. We have provided the open-source software code at Physionet (<https://physionet.org/physiotools/geh/>). In addition to previously reported “mean” GEH measures, [4] in this study we measured the spatial peak vectors (Fig. 1) [13–15]. First, we transformed the 12-lead ECG into an orthogonal XYZ ECG, using Kors transformation [16]. Next, we constructed a time-coherent median beat, and detected the origin of the heart vector using our novel approach, as recently described [14]. Then, we performed calculations of GEH metrics using the following equations.

Spatial QRS-T angles

Spatial peak QRS-T angle was calculated as the 3-dimensional angle between the spatial peak QRS vector and the spatial peak T vector:

$$Spatial\ peak\ QRS-T\ angle = \arccos\left(\frac{|\overrightarrow{QRSpeak} \cdot \overrightarrow{Tpeak}|}{|\overrightarrow{QRSpeak}| |\overrightarrow{Tpeak}|}\right) \tag{A.1}$$

Spatial area QRS-T angle was calculated as the 3-dimensional angle between the spatial area QRS vector and the spatial area T vector:

$$Spatial\ area\ QRS-T\ angle = \arccos\left(\frac{|\overrightarrow{QRSmean} \cdot \overrightarrow{Tmean}|}{|\overrightarrow{QRSmean}| |\overrightarrow{Tmean}|}\right) \tag{A.2}$$

Spatial ventricular gradient vectors:

Magnitude and direction of spatial area (Wilson’s) and peak SVG vectors were measured.

$$\overrightarrow{SVG} = \overrightarrow{QRSpeak} + \overrightarrow{Tpeak} \tag{A.3}$$

$$Spatial\ Peak\ SVG\ Azimuth = \arctan\left(\frac{SVG_V_Z dt}{SVG_V_X dt}\right) \tag{A.4}$$

$$Spatial\ Peak\ SVG\ Elevation = \arctan\left(\frac{SVG_V_X dt}{SVG_V_Y dt}\right) \tag{A.5}$$

$$SpatialPeakSVGMagnitude = \sqrt{SVG_V_X^2 + SVG_V_Y^2 + SVG_V_Z^2} \tag{A.6}$$

$$Spatial\ Area\ SVG\ Azimuth = \arctan\left(\frac{\int_{QRS-onset}^{T-offset} V_Z(t) dt}{\int_{QRS-onset}^{T-offset} V_X(t) dt}\right) \tag{A.7}$$

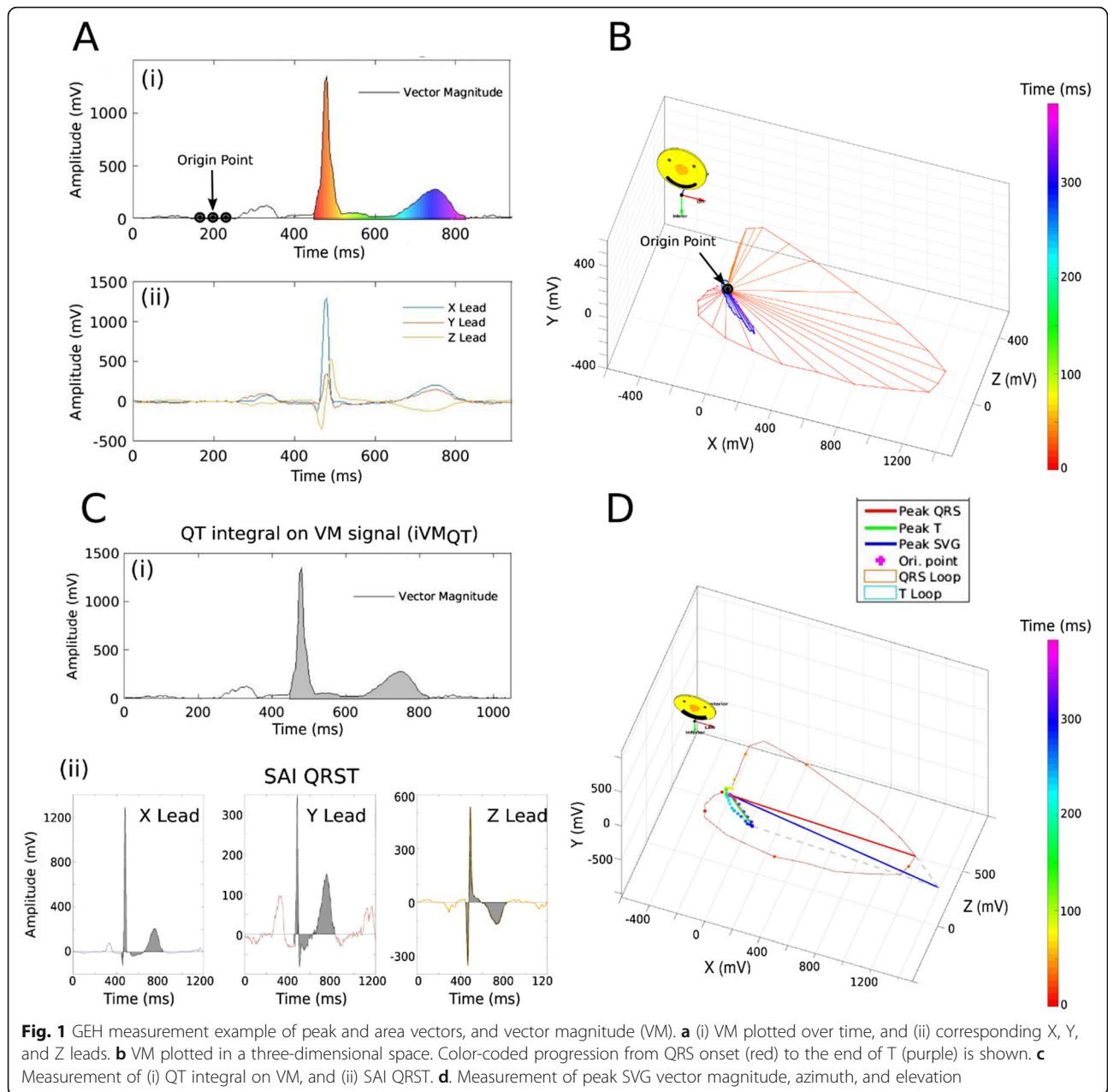
$$Spatial\ Area\ SVG\ Elevation = \arctan\left(\frac{\int_{QRS-onset}^{T-offset} V_X(t) dt}{\int_{QRS-onset}^{T-offset} V_Y(t) dt}\right) \tag{A.8}$$

Wilson’s (area) SVG magnitude was also calculated:

$$|SVG| = \sqrt{\left(\int_{QBeg}^{TEnd} V_x(t) dt\right)^2 + \left(\int_{QBeg}^{TEnd} V_y(t) dt\right)^2 + \left(\int_{QBeg}^{TEnd} V_z(t) dt\right)^2} \tag{A.9}$$

Statistical analysis

Time-dependent area under the receiver operating characteristic curve (ROC(t)AUC) analysis was performed to assess the predictive accuracy of a continuous biomarker in a period of 3, 6, 9 months, and 1,2,3,5,10, and 15 years, using an unadjusted survival analysis framework approach [17, 18]. We used the nearest neighbor estimator, which allows the censoring to depend on the marker and is therefore realistic. The percentage of observations included in each neighborhood was defined by the eq. $0.25^* (\sqrt[3]{n})$, where n is the number of observations. All available five visits’ ECG data were included in time-dependent AUC analysis [4]. To satisfy the requirement for ROC analysis, and to perform internal validation of study findings, we divided the dataset into five unique (non-overlapping) partitions. In each partition, a study participant was presented not more than once, with a unique time to event defined as time from ECG recording to the time of outcome (or censoring). If a participant had five ECGs recorded at five study visits, each ECG contributed to a different partition. Those participants who had less than 5 visits/ECGs were randomly distributed across 5 partitions. Bootstrapping with 500 replications was performed to determine a 95% confidence interval (CI) of ROC(t) AUC in each partition, separately. Then, ROC(t) AUC point estimates, and lower and upper boundaries of 95%CI were averaged across 5 partitions, then presented as a final summary result. To assess the statistical power of ROC(t) AUC analysis at each time period, we compared observed 95% CI width with expected 95% CI width. Expected 95% CI width was calculated for observed sample size and observed AUC values at each time period. We summarized clinical characteristics of study participants with an SCD outcome within the first 3 months, 3–6 months, 6 months-1 year, 1–2 years,



2–5 years, and more than 5 years after ECG recording in a longitudinal dataset, reporting between-participant standard deviation (SD) for continuous variables, and between-participant frequencies for categorical variables. We then assessed whether the addition of traditional ECG metrics (heart rate, QRS, QTc) and GEH metrics to our previously identified clinical risk factors of SCD [4] (age, sex, race, diabetes, hypertension, CHD, and stroke) resulted in better predictive accuracy for SCD and non-SCD within the first 3 months, 3–6 months, 6 months–1 year, 1–2 years, 2–5 years, and more than 5 years after ECG recording. We calculated absolute integrated discrimination improvement

(IDI), and net reclassification improvement (NRI) using multivariate logistic regression [19, 20]. IDI estimates improvement in average sensitivity and specificity. We estimated category-free NRI and two-category NRI for events, defining the high-risk category as a $\geq 25\%$ risk of SCD/non-SCD within the first 3 months, 3–6 months, and 6 months–1 year after ECG recording. The high-risk category for events occurring 1–2 years, 2–5 years, and more than 5 years after ECG recording was defined as $\geq 10\%$ risk of SCD/non-SCD. Statistical analysis was performed using STATA MP 15.1 (StataCorp LP, College Station, TX, USA). A *P*-value of < 0.05 was considered significant. PASS

2019 Power Analysis and Sample Size Software (NCSS, LLC, Kaysville, Utah, USA) was used for the calculations of the expected 95% CI width.

Results

Study population

The clinical characteristics of the study population are shown in Table 1. Approximately half of the study participants were female, and 73% were white. Average traditional ECG parameters were normal. During the SCD adjudication, the inter-reviewer agreement was 83.2%, and agreement across phases was 92.5%. Over a median follow-up of 24.4 years, there were 577 SCDs (incidence 1.76 (95%CI 1.63–1.91) per 1000 person-years), and 829 non-SCDs (incidence 2.54 (95%CI 2.37–2.71) per 1000 person-years). SCD victims who died within the first 3 months after ECG recording were more likely to be CVD-free white males with fewer prevalent CVD risk factors. In contrast, SCD victims who died more than 5 years after ECG recording had nearly equal probabilities of being male or female, white or non-white (Table 1).

Time-dependent AUC analyses of SCD and competing outcome

Detailed results for all 5 partitions are provided in Additional file 1 Table S1 and Figs. 2, 3, 4. Considering the results of robust validation analysis, no ECG biomarkers predicted SCD within 3 months after ECG recording. Forward-directed SVG azimuth was significant predictor in some, but not all partitions: peak SVG azimuth partition #1 AUC 0.828 (95%CI 0.709–0.947), and partition #2 AUC 0.727 (95%CI 0.712–0.742). Predicted 95%CI width (Table 2) indicated insufficient statistical power for prediction of SCD within 3 months after ECG recording for most ECG biomarkers. At 6 months, SVG elevation was the only short-term statistically significant biomarker of SCD (area SVG elevation AUC 0.706; 95%CI 0.526–0.886), which specifically predicted SCD, but did not predict non-SCD (Fig. 6c). Figure 6 illustrates trends in variations in SVG vector direction (azimuth and elevation) predicting SCD versus non-SCD within 9 months – 1 year after ECG recording, when upward, and more likely forward-directed SVG vector predicted SCD, whereas leaning backward-directed SVG predicted non-SCD. In contrast, long-term (2 years and beyond) predictors of SCD and non-SCD had many similarities. Wide spatial QRS-T angle and backward [towards left ventricle (LV)] – directed SVG vector predicted both SCD and non-SCD. The most accurate prediction of SCD was provided by ECG biomarkers recorded within 2 years before the outcome (Figs. 5, 6). Most ECG biomarkers predicted both mortality outcomes, with few exceptions. SVG magnitude did not

predict any outcome. At any time, heart rate and QTc were stronger predictors of non-SCD than SCD (Fig. 5). Neither heart rate nor QTc improved risk reclassification beyond traditional clinical risk factors of SCD (Table 3), whereas QRS duration improved reclassification of SCD risk for events occurring 2–5 years after ECG recording. Within the first 3 months after ECG recording, only SVG azimuth improved reclassification of the risk beyond traditional clinical risk factors (18% SCD events were reclassified from a low or intermediate-risk category to a high-risk category). All GEH metrics significantly improved reclassification of both SCD and non-SCD beyond clinical risk factors for events occurring at least 1 year after ECG recording (Table 3).

Comparison of area-based versus peak-based SVG and QRS-T angle measurements

SCD predictive accuracy of peak-vector-based versus area-based spatial QRS-T angle, SVG direction, and SVG magnitude was similar (Fig. 7), with a trend towards slightly better prediction by peak-vector-based QRS-T angle and SVG azimuth, as compared to area-based QRS-T angle and SVG azimuth metrics.

Internal validation Results of internal validation are shown in Additional file 1: Table S1 and Figs. 2, 3, 4. As expected, long-term prediction of SCD was consistent across all 5 study partitions, whereas short-term (within 3–9 months) prediction was unreliable for most ECG variables (except SVG elevation). Consistently, statistical power was reliably sufficient for ROC(t) AUC analyses for outcomes occurring at least 1 year after ECG recording, and beyond (Table 2).

Discussion

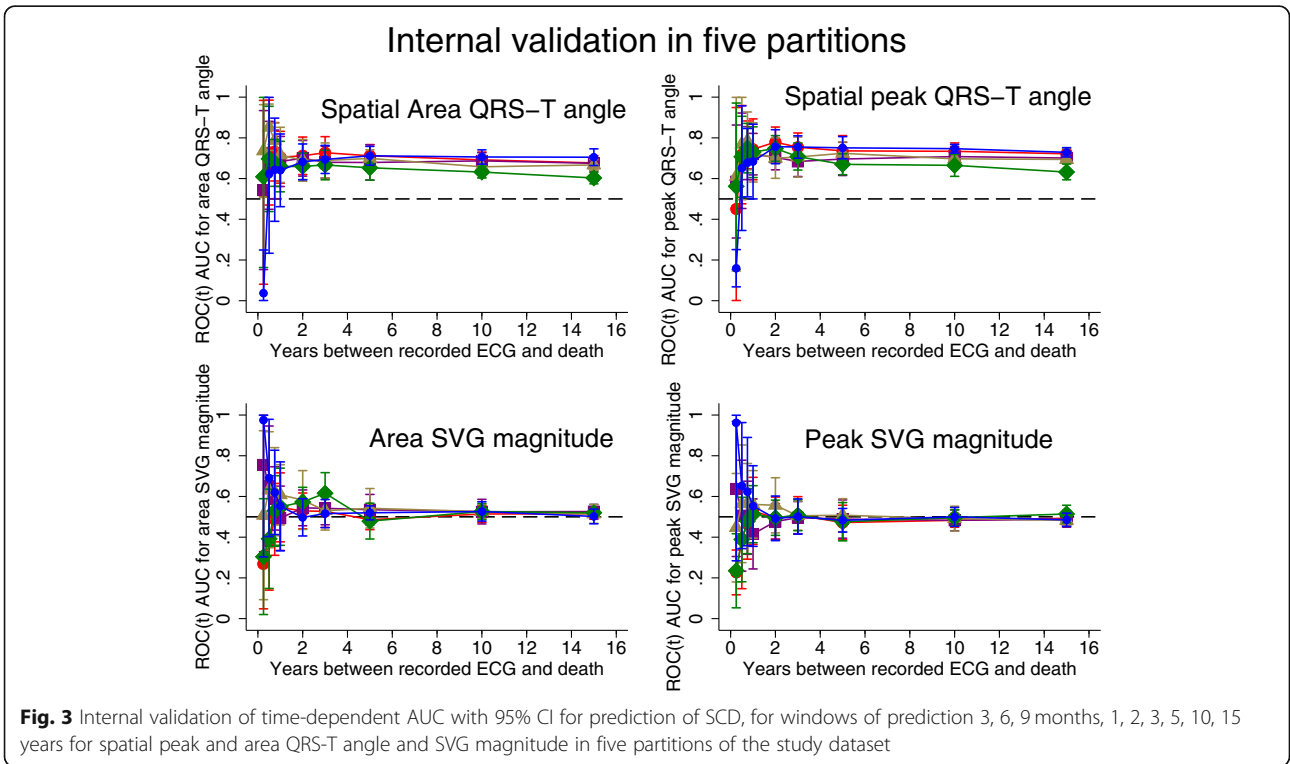
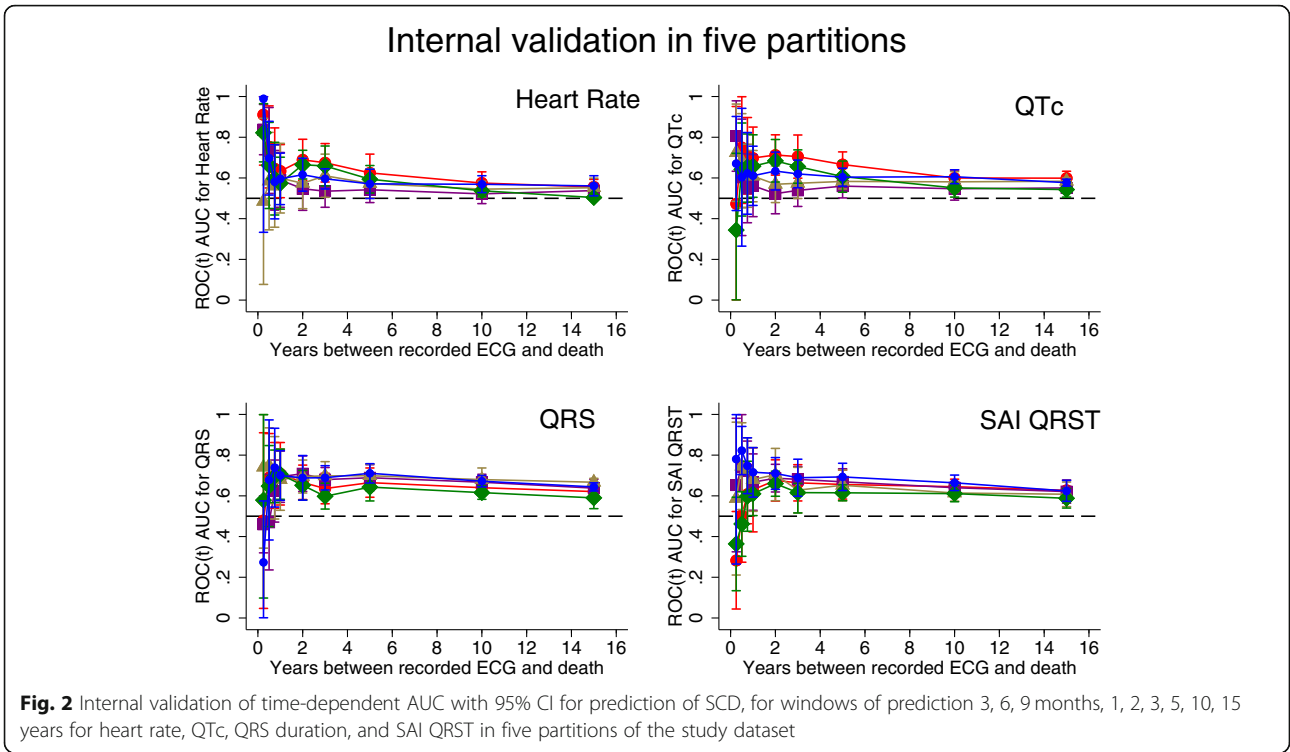
In this study, we described the dynamic predictive accuracy of ECG and VCG biomarkers of two competing mortality outcomes: SCD and non-SCD within a survival framework. Within the identified dynamic predictors of SCD, there was a distinction between markers predicting short-term events (within 6 months) and markers predicting more intermediate- and long-term events. This may represent the difference between markers heralding SCD (triggers or transient substrates) versus markers identifying persistent substrate. As expected, transient substrate of non-SCD (describing structural heart disease substrate) was characterized by wide QRS-T angle, SVG vector pointing backward (towards LV), wide QRS, prolonged QTc, and increased heart rate. A transient substrate of SCD was characterized by SVG vector pointing upward (towards the outflow tract). Dynamic predictive accuracy of ECG and VCG biomarkers of SCD should be taken into account for development of

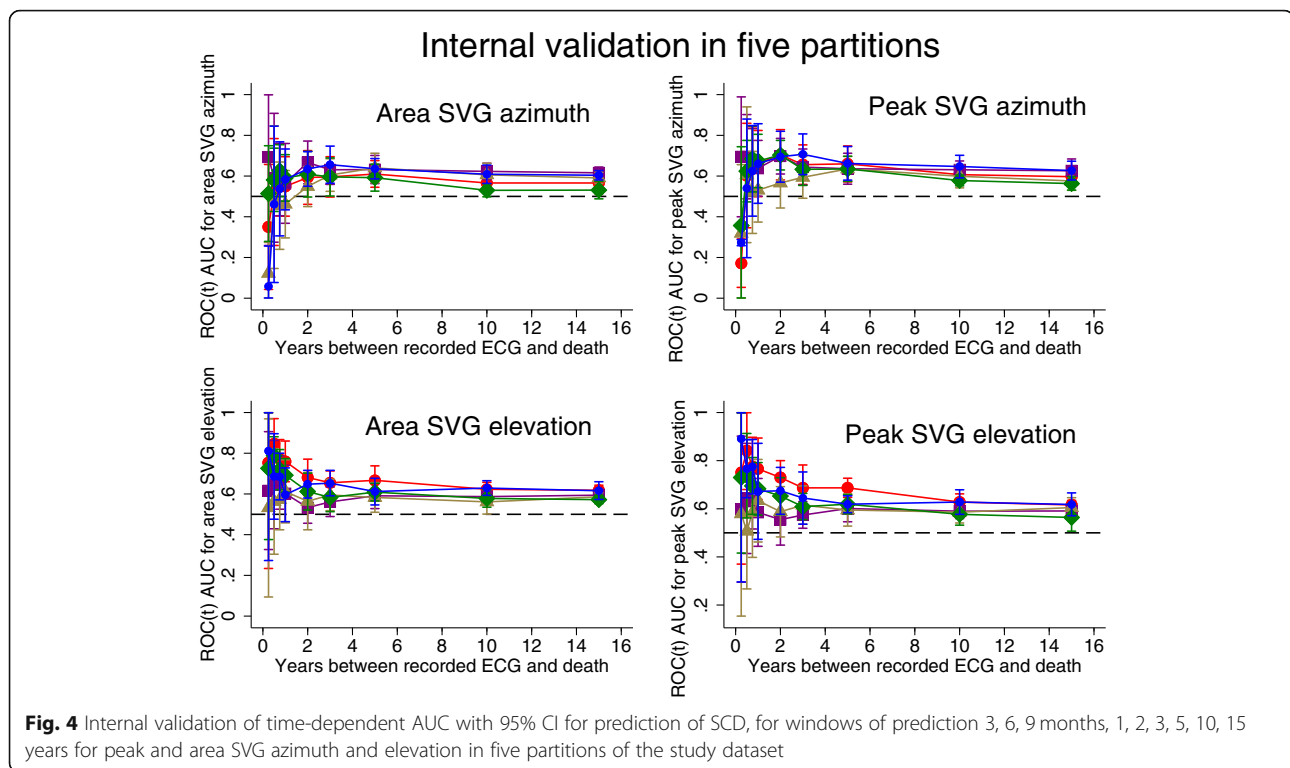
Table 1 Clinical characteristics of study population

SCD event within the following time interval after ECG recording:

Characteristic	n = 15,716	1–90 days (n = 11; T = 1)	91–180 days (n = 16; T = 1)	181–365 d (n = 47; T = 1)	365–730 d (n = 84; T = 1)	731–1825 d (n = 495; T = 2.5)	> 5 years (n = 320; T = 1.1)
Age ± SD, years	54.2 ± 5.8	63 ± 5	58 ± 6	62 ± 6	60 ± 7	59 ± 6	62 ± 7
Female, n(%)	8680(55.2)	18%	31%	30%	29%	36%	42%
White, n(%)	11431(72.7)	82%	50%	60%	60%	59%	56%
Diabetes, n(%)	1867(12.0)	40%	47%	39%	38%	39%	40%
Hypertension, n(%)	5475(35.0)	40%	60%	64%	68%	71%	68%
Anti-hypertensive drugs, n(%)	4803(30.6)	40%	53%	62%	70%	68%	66%
CHD, n(%)	756(4.8)	20%	33%	36%	39%	30%	25%
Heart failure, n(%)	732(4.7)	0	25%	15%	9%	10%	9%
Stroke, n(%)	269(1.7)	0	13%	7%	18%	10%	10%
Peripheral artery disease, n(%)	630(4.2)	0	0	14%	17%	9%	14%
Current smoking, n(%)	4107(26.2)	40%	47%	36%	39%	38%	29%
Body-mass-index±SD, kg/m ²	27.7 ± 5.4	32.4 ± 5.8	29.2 ± 5.4	29.1 ± 6.7	28.8 ± 6.2	29.4 ± 5.9	30.4 ± 6.6
Total cholesterol±SD, mmol/L	5.6 ± 1.1	5.3 ± 0.8	5.0 ± 1.2	5.2 ± 1.2	5.2 ± 1.2	5.6 ± 1.0	5.3 ± 1.1
Triglycerides±SD, mmol/L	1.5 ± 1.0	2.3 ± 2.0	1.5 ± 0.7	1.7 ± 1.1	1.9 ± 1.5	1.7 ± 1.2	1.7 ± 1.2
Alcohol consumption±SD, g/wk	42.4 ± 97.0	11 ± 23	130 ± 390	28 ± 75	44 ± 94	46 ± 102	33 ± 76
Heart rate ± SD, bpm	66.3 ± 10.3	74 ± 13	68 ± 11	65 ± 10	69 ± 14	67 ± 10	66 ± 12
Corrected QT ± SD, ms	416.4 ± 19.7	428 ± 20	436 ± 44	429 ± 33	433 ± 35	423 ± 23	424 ± 22
QRS duration±SD, ms	92.3 ± 12.7	97 ± 16	99 ± 12	109 ± 24	105 ± 24	98 ± 18	98 ± 18
BBB/IVCD, n(%)	666(4.2)	9%	6%	19%	13%	12%	12%
LBBB, n(%)	111(0.7)	4.5%	3.1%	2.7%	3.0%	1.0%	1.2%

T average number of visits (ECGs) per participant





dynamic and life-long prediction of SCD and non-SCD. Importantly, the addition of GEH metrics (but not QTc) to known demographic and clinical risk factors (age, sex, race, CHD, stroke, diabetes, and hypertension) significantly improved reclassification of risk, supporting inclusion of GEH metrics into dynamic risk scores for SCD.

Triggers, or transient substrate of SCD event

An SCD event represents a “perfect storm,” requiring both susceptible anatomical/functional substrate and a trigger/transient initiating event [21]. Short-term predictors of SCD in our study reflect possible SCD triggers. The SVG vector direction predicting short-term SCD risk differed from SVG vector direction of the intermediate- and long-term risk of SCD. The short-term risk was uniquely predicted by an SVG vector pointing upward (toward the outflow tract), suggesting that short total recovery time in the outflow tracts (as the SVG vector points towards an area with the shortest total refractory time) [22] may represent an SCD trigger. SVG azimuth was the only ECG metric which improved reclassification of the risk beyond known clinical and demographic risk factors. Indeed, it is known that “malignant” idiopathic ventricular fibrillation and polymorphic ventricular tachycardia can be triggered by ventricular ectopy arising from the outflow tracts [23]. Early cardiac development affects the generation of electrophysiological heterogeneities in the adult heart [24]. There may be a

genetic basis for this phenomenon as GEH-associated genetic polymorphisms indicated the involvement of *HAND1* and *TBX3* genes [5], both of which play a role in outflow tract development.

Intermediate and long-term substrates of SCD

All ECG measurements (except SVG magnitude) predicted SCD long-term. The long-term substrate of SCD was characterized by an SVG vector pointing backward (toward the LV), a wide spatial QRS-T angle, and a large SAI QRST. Reliable long-term prediction of SCD offers an opportunity for early preventive intervention. Many GEH-associated genetic loci are implicated in cardiac development [5]. Further studies of the underlying biology behind GEH-associated loci will help to uncover novel mechanisms of SCD and develop primary prevention strategies. A recent case-control genome-wide association study of sudden cardiac arrest [25] did not identify any variants at genome-wide statistical significance. An ideal case-control study of paroxysmal life-threatening arrhythmias (e.g. SCD) would require evidence of freedom from arrhythmogenic substrate in controls, which is difficult to achieve. As both trigger and substrate are required for the development of sudden cardiac arrest, a low yield from a case-control genome-wide association study of sudden cardiac arrest is to be expected. In contrast, genomic studies of electrophysiological substrates have the advantage of a more accurate measurement of phenotype and larger statistical

Table 2 Calculated/predicted and observed two-sided 95% confidence interval width for a range of observed AUC values

Time	N events	n non-events	ECG predictor	ROC AUC	Calculated / predicted			Observed		
					95%CI width	Lower CI limit	Upper CI limit	ROC AUC	Lower CI limit	Upper CI limit
3 months	11	15,705	HR	0.809	0.311	0.654	0.964	0.809	0.493	0.963
			QTc	0.604	0.355	0.427	0.781	0.604	0.312	0.903
			QRS	0.506	0.343	0.335	0.677	0.506	0.162	0.817
			pQRST	0.473	0.335	0.306	0.640	0.473	0.135	0.807
			pSVGaz	0.363	0.293	0.216	0.510	0.363	0.143	0.594
			pSVGel	0.71	0.346	0.537	0.883	0.71	0.306	0.98
			pSVGmag	0.502	0.342	0.331	0.673	0.502	0.189	0.687
			aQRST	0.492	0.339	0.322	0.662	0.492	0.181	0.826
			aSVGaz	0.347	0.286	0.204	0.490	0.347	0.117	0.587
			aSVGel	0.688	0.350	0.513	0.863	0.688	0.261	0.974
			aSVGmag	0.562	0.352	0.386	0.738	0.562	0.159	0.8
6 months	16	15,700	SAIQRST	0.534	0.346	0.360	0.708	0.534	0.196	0.812
			HR	0.686	0.290	0.541	0.831	0.686	0.477	0.895
			QTc	0.656	0.293	0.509	0.803	0.656	0.385	0.923
			QRS	0.647	0.294	0.500	0.794	0.647	0.421	0.873
			pQRST	0.706	0.288	0.556	0.844	0.706	0.456	0.949
			pSVGaz	0.613	0.294	0.466	0.760	0.613	0.356	0.871
			pSVGel	0.699	0.288	0.556	0.844	0.699	0.514	0.883
			pSVGmag	0.5	0.283	0.358	0.642	0.5	0.236	0.765
			aQRST	0.713	0.286	0.570	0.856	0.713	0.466	0.957
			aSVGaz	0.53	0.289	0.390	0.678	0.53	0.237	0.824
			aSVGel	0.706	0.287	0.562	0.850	0.706	0.526	0.886
1 year	47	15,669	aSVGmag	0.549	0.292	0.416	0.708	0.549	0.279	0.819
			SAIQRST	0.655	0.293	0.509	0.803	0.655	0.454	0.85
			HR	0.598	0.172	0.512	0.684	0.598	0.461	0.737
			QTc	0.628	0.172	0.542	0.714	0.628	0.482	0.774
			QRS	0.698	0.168	0.614	0.784	0.698	0.563	0.833
			pQRST	0.721	0.166	0.638	0.805	0.721	0.58	0.862
			pSVGaz	0.633	0.172	0.547	0.719	0.633	0.477	0.79
			pSVGel	0.668	0.171	0.583	0.753	0.668	0.518	0.818
			pSVGmag	0.514	0.167	0.431	0.597	0.514	0.346	0.683
			aQRST	0.681	0.170	0.596	0.766	0.681	0.543	0.819
			aSVGaz	0.55	0.170	0.465	0.635	0.55	0.396	0.704
2 years	84	15,632	aSVGel	0.652	0.171	0.566	0.738	0.652	0.531	0.774
			aSVGmag	0.55	0.170	0.465	0.635	0.55	0.373	0.726
			SAIQRST	0.661	0.171	0.576	0.746	0.661	0.515	0.807
			HR	0.618	0.129	0.554	0.682	0.618	0.522	0.715
			QTc	0.625	0.129	0.561	0.689	0.625	0.528	0.722
			QRS	0.682	0.127	0.618	0.746	0.682	0.595	0.769
			pQRST	0.738	0.123	0.677	0.799	0.738	0.661	0.814
			pSVGaz	0.673	0.127	0.609	0.737	0.673	0.567	0.779
			pSVGel	0.64	0.128	0.576	0.704	0.64	0.549	0.731
			pSVGmag	0.503	0.124	0.441	0.565	0.503	0.399	0.608

Table 2 Calculated/predicted and observed two-sided 95% confidence interval width for a range of observed AUC values (Continued)

Time	N events	n non-events	ECG predictor	ROC AUC	Calculated / predicted			Observed		
					95%CI width	Lower CI limit	Upper CI limit	ROC AUC	Lower CI limit	Upper CI limit
5 years	495	15,221	aQRST	0.689	0.127	0.626	0.752	0.689	0.602	0.776
			aSVGaz	0.611	0.129	0.547	0.675	0.611	0.504	0.717
			aSVGel	0.608	0.129	0.544	0.672	0.608	0.515	0.701
			aSVGmag	0.545	0.127	0.482	0.608	0.545	0.448	0.642
			SAIQRST	0.687	0.127	0.624	0.750	0.687	0.600	0.775
			HR	0.581	0.053	0.554	0.608	0.581	0.508	0.654
			QTc	0.604	0.054	0.577	0.631	0.604	0.548	0.659
			QRS	0.681	0.053	0.655	0.717	0.681	0.62	0.743
			pQRST	0.715	0.052	0.689	0.741	0.715	0.652	0.779
			pSVGaz	0.646	0.053	0.619	0.673	0.646	0.572	0.72
			pSVGel	0.624	0.054	0.597	0.651	0.624	0.577	0.671
			pSVGmag	0.486	0.051	0.460	0.512	0.486	0.403	0.568
			aQRST	0.691	0.053	0.665	0.717	0.691	0.633	0.749
			aSVGaz	0.622	0.054	0.595	0.649	0.622	0.557	0.687
			aSVGel	0.612	0.054	0.585	0.639	0.612	0.549	0.675
aSVGmag	0.512	0.052	0.486	0.538	0.512	0.444	0.581			
SAIQRST	0.657	0.053	0.630	0.684	0.657	0.594	0.72			
> 5 years	320	15,396	HR	0.55	0.066	0.517	0.583	0.55	0.507	0.593
			QTc	0.577	0.066	0.544	0.610	0.577	0.532	0.622
			QRS	0.655	0.066	0.622	0.688	0.655	0.617	0.693
			pQRST	0.71	0.064	0.678	0.742	0.71	0.668	0.753
			pSVGaz	0.612	0.066	0.579	0.645	0.612	0.567	0.657
			pSVGel	0.602	0.066	0.567	0.633	0.602	0.561	0.643
			pSVGmag	0.491	0.064	0.459	0.523	0.491	0.444	0.537
			aQRST	0.675	0.066	0.642	0.708	0.675	0.636	0.714
			aSVGaz	0.587	0.066	0.554	0.610	0.587	0.544	0.629
			aSVGel	0.596	0.066	0.563	0.629	0.596	0.555	0.636
			aSVGmag	0.523	0.065	0.491	0.555	0.523	0.479	0.568
			SAIQRST	0.635	0.066	0.602	0.668	0.635	0.598	0.672

power (as an outcome is a continuous variable), providing higher yield.

Dynamic predictive accuracy of biomarkers within a survival framework

The dynamic nature of SCD risk is well-recognized. However, the dynamic predictive accuracy of SCD risk markers has not been previously studied. Our large prospective epidemiological study used repeated ECG measures, obtained at five follow-up visits, which ensured stable estimates of the dynamic predictive accuracy of ECG biomarkers within a survival framework. An analytical framework for the assessment of a dynamic predictive accuracy of biomarkers for censored survival data

was developed fairly recently [17]. Heagerty et al. [17] showed that a simple estimator based on Kaplan-Meier method has serious shortcomings for characterization of accuracy for censored survival outcomes, and developed the nearest neighbor estimator as a valid ROC solution for prediction accuracy assessment, allowing the censoring process to depend on the marker. In this study, we used an analytical approach to answer an agnostic predictive accuracy question. To mimic the real-life clinical scenarios, we intentionally did not adjust for confounders and therefore did not comment on the independence of association of ECG biomarkers with SCD at any given time point. There were noticeable differences in the clinical characteristics of study participants who

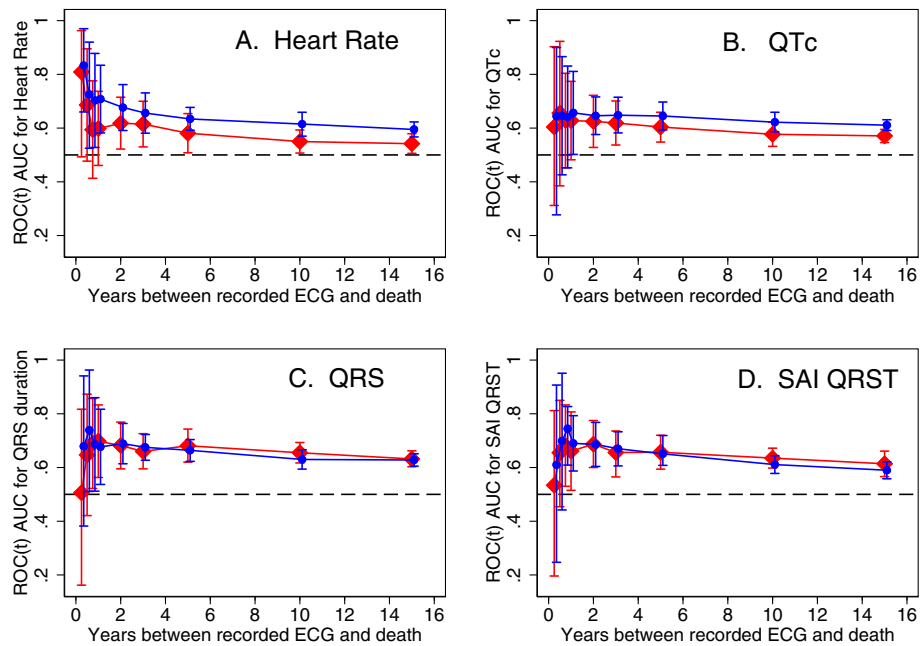


Fig. 5 Time-dependent AUC with 95% CI for prediction of SCD (red diamonds), and non-SCD (blue circles) for windows of prediction 3, 6, 9 months, 1, 2, 3, 5, 10, 15 years for (a) heart rate, (b) QTc interval, (c) QRS duration, (d) SAI QRST measured at visits 1, 2, 3, 4, and 5

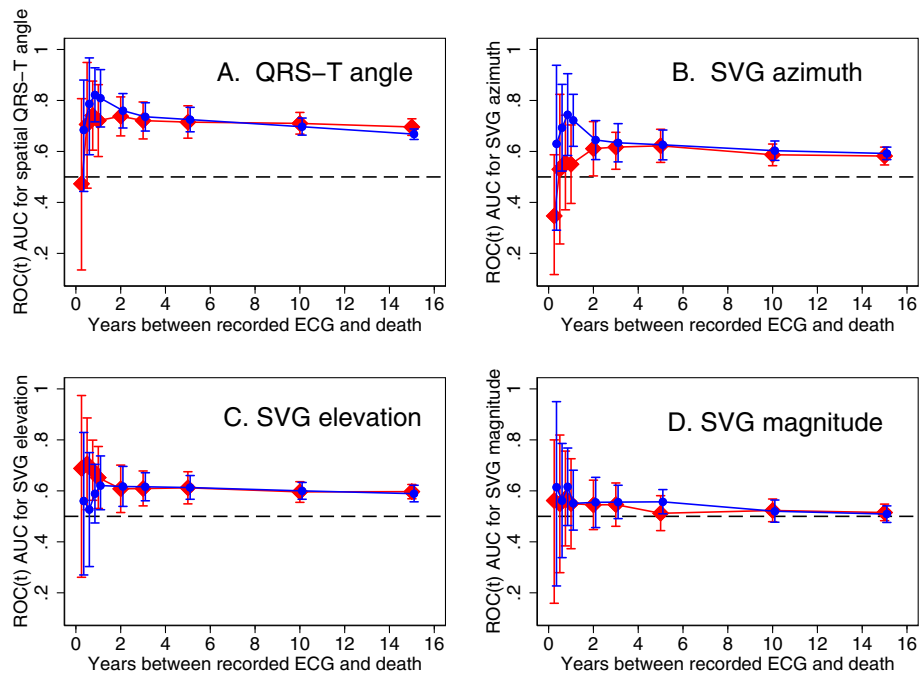


Fig. 6 Time-dependent AUC with 95% CI for prediction of SCD (red diamonds), and non-SCD (blue circles) for windows of prediction 3, 6, 9 months, 1, 2, 3, 5, 10, 15 years for (a) spatial peak QRS-T angle, (b) area SVG azimuth, (c) area SVG elevation, (d) area SVG magnitude measured at visits 1, 2, 3, 4, and 5

Table 3 Integrated Discrimination Improvement (IDI) and Net Reclassification Improvement (NRI) for ECG metrics added to clinical predictors of SCD and nonSCD outcomes (age, sex, race, coronary heart disease, stroke, hypertension, diabetes)

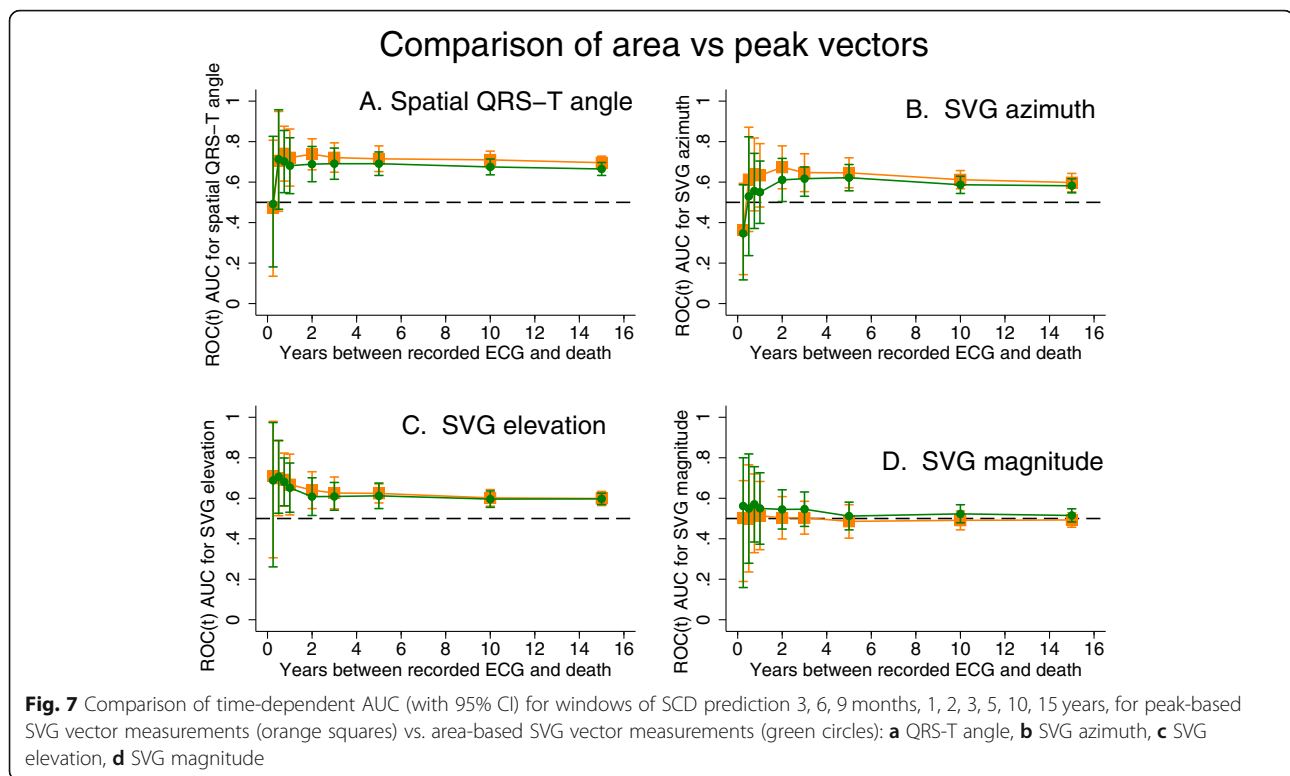
Outcome	Prediction model	Reclassification index	1–90 days (high risk ≥25%)	91–180 d (high risk ≥25%)	181–365 d (high risk ≥25%)	365–730 d (high risk ≥10%)	731–1825 d (high risk ≥10%)	> 5 years (high risk ≥10%)
Sudden cardiac death	Clinical + QTc, ms	Absolute IDI (P-value)	0.063(0.109)	0.007(0.437)	0.001(0.695)	0.004(0.236)	0.001(0.020)	0.0003(0.424)
		Event Reclassified Up	2/11(18%)	0	2/47(4.3%)	3/84(3.6)	11/495(2%)	0
		Category-free NRI (P-value)	0.331(0.106)	-0.049(0.473)	0.057(0.114)	0.011(0.677)	0.005(0.226)	-0.003(0.432)
Clinical + QRS, ms	Clinical + QRS, ms	Absolute IDI (P-value)	0.012(0.430)	0.004(0.785)	0.013(0.097)	0.003(0.215)	0.002(0.00006)	0.001(0.070)
		Event Reclassified Up	0	0	0	3/84(3.6%)	19/495(3.8%)	1/320(0.3%)
		Category-free NRI (P-value)	-0.023(0.839)	-0.015(0.853)	0.058(0.018)	0.003(0.919)	0.009(0.032)	-0.009(0.198)
Clinical + heart rate, bpm	Clinical + heart rate, bpm	Absolute IDI (P-value)	0.00004(0.978)	0.026(0.244)	0.020(0.030)	0.0003(0.664)	-0.0002(0.402)	0.0005(0.410)
		Event Reclassified Up	0	0	4/47(8.5%)	3/84(3.6%)	11/495(2.2%)	3/320(1%)
		Category-free NRI (P-value)	0(1.0)	-0.067(0.420)	0.029(0.671)	0.034(0.109)	0.003(0.433)	-0.004(0.630)
Clinical+ Area QRS-T angle, °	Clinical+ Area QRS-T angle, °	Absolute IDI (P-value)	0.001(0.784)	0.066(0.046)	0.0001(0.852)	0.005(0.195)	0.005(< 0.00001)	0.002(0.029)
		Event Reclassified Up	0	1/16(6.3%)	0	2/84(2.4%)	46/495(9.6%)	1/320(0.3%)
		Category-free NRI (P-value)	0(1.0)	-0.032(0.801)	-0.006(0.317)	0.035(0.118)	0.021(0.003)	-0.006(0.308)
Clinical+ Peak QRS-T angle, °	Clinical+ Peak QRS-T angle, °	Absolute IDI (P-value)	0.032(0.328)	0.048(0.083)	-0.00001(0.986)	0.007(0.084)	0.007(< 0.00001)	0.001(0.045)
		Event Reclassified Up	2/11(18%)	1/16(6.3%)	0	5/84(6.0)	52/495(10.5%)	1/320(0.3%)
		Category-free NRI (P-value)	0.216(0.246)	-0.101(0.420)	-0.012(0.157)	0.041(0.252)	0.021(0.006)	-0.015(0.067)
Clinical+ Area SVG azimuth, °	Clinical+ Area SVG azimuth, °	Absolute IDI (P-value)	0.012(0.607)	0.007(0.651)	0.002(0.665)	0.020(0.001)	0.002(0.004)	-0.0002(0.00008)
		Event Reclassified Up	2/11(18%)	0	1/47(2.1%)	7/84(7.1%)	21/495(4.2%)	0
		Category-free NRI (P-value)	0.277(0.068)	-0.050(0.541)	0.023(0.398)	0.055(0.152)	0.003(0.578)	0.0002(0.083)
Clinical+ Peak SVG azimuth, °	Clinical+ Peak SVG azimuth, °	Absolute IDI (P-value)	0.015(0.608)	0.045(0.141)	-0.0001(0.880)	0.017(0.005)	0.003(0.00005)	-0.0001(0.568)
		Event Reclassified Up	2/11(18%)	0	0	5/84(6%)	27/495(5.5%)	0
		Category-free NRI (P-value)	0.277(0.068)	-0.133(0.221)	-0.006(0.564)	0.020(0.598)	0.004(0.538)	0.0009(0.003)
Clinical + Area SVG elevation, °	Clinical + Area SVG elevation, °	Absolute IDI (P-value)	0.002(0.735)	0.050(0.063)	0.004(0.398)	-0.00001(0.990)	0.0001(0.576)	-0.0004(0.045)
		Event Reclassified Up	0	1/16(6.3%)	0	3/84(3.6%)	11/495(2.2%)	0
		Category-free NRI (P-value)	0.038(0.317)	-0.118(0.349)	0.018(0.257)	0.037(0.093)	0.001(0.847)	0.0004(0.034)
Clinical + Peak SVG elevation, °	Clinical + Peak SVG elevation, °	Absolute IDI (P-value)	0.003(0.663)	0.046(0.112)	0.002(0.463)	0.0004(0.879)	0.0002(0.387)	-0.0003(0.023)
		Event Reclassified Up	0	0	0	5/84(6%)	7/495(1.4%)	0

Table 3 Integrated Discrimination Improvement (IDI) and Net Reclassification Improvement (NRI) for ECG metrics added to clinical predictors of SCD and nonSCD outcomes (age, sex, race, coronary heart disease, stroke, hypertension, diabetes) (Continued)

Outcome	Prediction model	Reclassification index	1–90 days (high risk ≥25%)	91–180 d (high risk ≥25%)	181–365 d (high risk ≥25%)	365–730 d (high risk ≥10%)	731–1825 d (high risk ≥10%)	> 5 years (high risk ≥10%)
Non-Sudden cardiac death	Clinical + SAI QRS-T mV*ms	Category-free NRI (P-value)	0.038(0.317)	-0.084(0.276)	0.006(0.564)	0.070(0.017)	-0.004(0.240)	0.0005(0.020)
		Absolute IDI (P-value)	0.0001(0.755)	0.023(0.339)	0.002(0.522)	0.012(0.040)	0.002(0.0004)	0.001(0.061)
	Clinical + SVG magnitude, µV	Event Reclassified Up	0	0	0	1/84(1.2%)	23/495(4.6%)	1/320(0.3%)
		Category-free NRI (P-value)	0(1.0)	-0.151(0.151)	0.006(0.564)	0.007(0.778)	0.013(0.0005)	0.0005(0.909)
	Clinical + Peak SVG mag, µV	Absolute IDI (P-value)	0.015(0.566)	-0.0002(0.954)	0.0002(0.884)	0.0009(0.188)	-0.0002(0.00003)	0.00007(0.764)
		Event Reclassified Up	0	0	0	2/84(2.4%)	0	0
Clinical + QTc, ms	Category-free NRI (P-value)	-0.023(0.839)	-0.052(0.083)	-0.012(0.157)	0.018(0.318)	0.0001(0.371)	-0.002(0.516)	
	Absolute IDI (P-value)	0.001(0.748)	0.0003(0.959)	0.0002(0.869)	0.0006(0.095)	-0.00006(0.676)	-0.0002(0.189)	
Clinical + QRS, ms	Event Reclassified Up	0	0	0	3/84(3.6%)	7/495(1.4%)	0	
	Category-free NRI (P-value)	0(1.0)	-0.052(0.180)	-0.012(0.157)	0.032(0.135)	0.004(0.144)	0.0003(0.102)	
Clinical + heart rate, bpm	Absolute IDI (P-value)	0.069(0.170)	0.006(0.667)	0.015(0.200)	0.0001(0.843)	0.003(< 0.00001)	0.001(0.040)	
	Event Reclassified Up	0	0	2/47(2.3%)	0	46/711(6.5%)	10/394(2.5%)	
Clinical+ Area QRS-T angle, °	Category-free NRI (P-value)	0.200(0.059)	0(1.0)	-0.006(0.880)	-0.01(0.225)	0.002(0.749)	0.016(0.064)	
	Absolute IDI (P-value)	0.028(0.467)	0.187(0.001)	-0.002(0.702)	0.0007(0.623)	0.002(0.0001)	0.001(0.051)	
Clinical+ Peak QRS-T angle, °	Event Reclassified Up	0	2/16(12.5%)	0	0	34/711(4.8%)	10/394(2.5%)	
	Category-free NRI (P-value)	-0.011(0.919)	0.136(0.230)	0.014(0.561)	0.011(0.225)	0.004(0.395)	0.009(0.337)	
Clinical+ Area QRS-T angle, °	Absolute IDI (P-value)	0.060(0.160)	-0.0001(0.981)	0.0005(0.909)	0.0003(0.779)	0.005(< 0.00001)	0.002(0.010)	
	Event Reclassified Up	0	0	1/47(2.1%)	0	89/711(12.5%)	14/394(3.6%)	
Clinical+ Peak QRS-T angle, °	Category-free NRI (P-value)	0.200(0.059)	0(1.0)	0.037(0.158)	-0.0002(0.990)	0.014(0.060)	0.014(0.207)	
	Absolute IDI (P-value)	0.053(0.272)	0.012(0.625)	0.059(0.002)	0.007(0.120)	0.010(< 0.00001)	0.004(0.0004)	
Clinical+ Peak QRS-T angle, °	Event Reclassified Up	1/11(9%)	0	4/47(8.5%)	0	108/711(15%)	19/394(4.8%)	
	Category-free NRI (P-value)	0.120(0.411)	-0.049(0.499)	0.060(0.286)	0.084(0.0003)	0.017(0.034)	0.021(0.097)	
Clinical+ Peak QRS-T angle, °	Absolute IDI (P-value)	0.169(0.026)	0.077(0.030)	0.072(0.0004)	0.005(0.180)	0.009(< 0.00001)	0.005(0.00002)	
	Event Reclassified Up	1/11(9%)	0	6/47(12.8%)	0	114/711(16%)	24/394(6.1%)	
Category-free NRI (P-value)	0.120(0.411)	-0.084(0.276)	0.01(0.167)	0.052(0.006)	0.017(0.033)	0.034(0.011)		

Table 3 Integrated Discrimination Improvement (IDI) and Net Reclassification Improvement (NRI) for ECG metrics added to clinical predictors of SCD and nonSCD outcomes (age, sex, race, coronary heart disease, stroke, hypertension, diabetes) (Continued)

Outcome	Prediction model	Reclassification index	1–90 days (high risk ≥25%)	91–180 d (high risk ≥25%)	181–365 d (high risk ≥25%)	365–730 d (high risk ≥10%)	731–1825 d (high risk ≥10%)	> 5 years (high risk ≥10%)
Clinical+ Area SVG azimuth, °	Absolute IDI (P-value)	0.183(0.003)	0.123(0.010)	0.014(0.093)	0.0008(0.534)	0.003(< 0.00001)	0.003(0.0006)	
	Event Reclassified Up	1/11(9%)	0	1/47(2.1%)	0	57/71(8.0%)	13/394(3.3%)	
	Category-free NRI (P-value)	0.200(0.202)	-0.049(0.574)	-0.005(0.899)	-0.0002(0.994)	0.009(0.109)	0.06(0.112)	
Clinical+ Peak SVG azimuth, °	Absolute IDI (P-value)	0.164(0.015)	0.005(0.740)	0.007(0.315)	0.0003(0.642)	0.003(< 0.00001)	0.003(0.001)	
	Event Reclassified Up	1/11(9%)	0	2/47(2.3%)	0	45/71(6.3%)	17/394(4.3%)	
	Category-free NRI (P-value)	0.240(0.138)	0.017(0.317)	-0.008(0.840)	-0.002(0.782)	0.003(0.600)	0.027(0.019)	
Clinical + Area SVG elevation, °	Absolute IDI (P-value)	0.025(0.398)	0.058(0.057)	0.007(0.370)	0.0008(0.356)	0.0005(0.015)	0.0006(0.044)	
	Event Reclassified Up	0	0	4/47(8.5%)	0	16/71(2.3%)	9/394(2.3%)	
	Category-free NRI (P-value)	-0.051(0.608)	0(1.0)	0.114(0.007)	-0.007(0.549)	-0.005(0.216)	0.018(0.025)	
Clinical + Peak SVG elevation, °	Absolute IDI (P-value)	0.039(0.273)	0.017(0.193)	0.018(0.081)	0.0005(0.703)	0.002(0.00007)	0.0004(0.081)	
	Event Reclassified Up	1/11(9%)	0	4/47(8.5%)	0	34/71(4.8%)	4/394(1.0%)	
	Category-free NRI (P-value)	0.189(0.319)	0.017(0.317)	0.068(0.210)	0.014(0.221)	-0.002(0.743)	0.009(0.065)	
Clinical + SAI QRST, mV*ms	Absolute IDI (P-value)	0.040(0.422)	0.018(0.528)	0.027(0.059)	0.019(0.022)	0.004(< 0.00001)	0.0006(0.093)	
	Event Reclassified Up	0	0	4/47(8.5%)	1/84(1%)	49/71(6.9%)	3/394(0.8%)	
	Category-free NRI (P-value)	0.109(0.392)	-0.084(0.251)	0.054(0.290)	0.098(0.003)	0.002(0.770)	0.003(0.580)	
Clinical + SVG magnitude, µV	Absolute IDI (P-value)	0.028(0.332)	-0.002(0.886)	-0.002(0.480)	0.026(0.004)	0.0008(0.00008)	0.0002(0.00008)	
	Event Reclassified Up	0	0	0	1/84(1%)	10/71(1.4%)	0	
	Category-free NRI (P-value)	0.029(0.799)	0(1.0)	0.006(0.317)	0.090(0.021)	-0.004(0.178)	-0.0004(0.059)	
Clinical + Peak SVG mag, µV	Absolute IDI (P-value)	0.027(0.355)	0.020(0.433)	-0.0004(0.907)	0.016(0.032)	0.0002(< 0.00001)	0.0003(0.067)	
	Event Reclassified Up	0	0	0	1/84(1%)	2/71(0.3%)	3/394(0.8%)	
	Category-free NRI (P-value)	0.029(0.799)	-0.067(0.348)	0(1.0)	0.098(0.005)	-0.001(0.473)	0.004(0.482)	



died suddenly within 3 months after ECG recording, as compared to those who experienced SCD 5 years after ECG recording. Nevertheless, observed dissimilarities in a dynamic predictive accuracy of ECG biomarkers suggested different mechanisms behind short-term SCD triggers (or transient substrates) and long-term SCD substrates. A study of SCD triggers is objectively difficult to conduct. The methodological approach of the dynamic predictive accuracy of ECG biomarkers within the survival framework can provide unique perspective on transient substrates and triggers of SCD, which prompts further investigation.

Global electrical heterogeneity

The GEH concept is based on Wilson's ventricular gradient [22, 26]. SVG defines a vector that characterizes the magnitude and direction of the steepest gradient between the longest and the shortest total recovery time across the entire heart, both left and right ventricles [27]. SVG vector is directed towards a zone with the shortest total recovery time. Therefore, GEH is a global measure of the dispersion of total recovery time across the heart, a marker of an underlying arrhythmogenic substrate, encompassing dispersion in both activation and refractoriness. We comprehensively characterize GEH by measuring five features of the SVG vector (Fig. 1): SVG magnitude, SVG direction (azimuth and

elevation), QRS-T angle, and SVG's scalar SAI QRST. The spatial QRS-T angle [28] is a well-known marker of the risk of SCD and cardiovascular mortality. SAI QRST is a scalar analog of the SVG [15, 29–31], associated with ventricular tachyarrhythmias in heart failure [29, 30, 32]. We previously showed that GEH is associated with SCD after adjustment for traditional ECG metrics and a comprehensive list of cardiovascular risk factors [4]. Five GEH metrics only weekly correlate with each other and traditional ECG measures, [5] and, therefore, are well-suited for inclusion in SCD risk scores. Importantly, GEH genome-wide association study [5] provided first clues about underlying biology behind GEH, which can lead to the future development of novel methods of SCD prevention. In vectorcardiography, there are two major approaches to define spatial vectors: either measuring spatial peak or area vectors [28]. In our study, some peak-based GEH metrics outperformed area-based GEH metrics. This finding may be at least partially explained by the fact that we used a physiologically sound definition of the heart vector origin point and time-coherent global median beat [14], which permitted accurate measurement of peak vectors. GEH metrics are highly reproducible [33], which is an essential factor for their future implementation in clinical practice. Of note, GEH can be calculated using 12-lead ECG that was recorded by any manufacturer ECG machine. The open-

source software code for GEH calculation is provided at <https://github.com/Tereshchenkolab/Origin> and <https://www.physionet.org/content/geh>.

Clinical implications

Our study is the first step towards the development of dynamic SCD risk prediction. Recently, we developed an SCD risk score [4], available at www.ecgpredictscd.org. However, our SCD risk model, similarly to other risk models [34, 35], includes risk factors that were measured once at baseline. Further improvement of SCD risk stratification requires knowledge of the dynamic predictive accuracy of ECG biomarkers of SCD. After validation of our study findings in another cohort, recommendations regarding an optimal frequency of ECG recordings can be developed.

Strengths and limitations

The strength of our study derives from the large prospective cohort design, with five longitudinal ECG recordings, long-term (median 24 years) follow-up, and a well-adjudicated SCD outcome. However, limitations of the study should be taken into account. The small number of events within 3 and 6 months after ECG recording limited the statistical power of SCD trigger analyses. It is worth noting that 9 out of 11 ARIC participants who succumbed to SCD within 3 months after ECG recording were men. We cannot rule out the possibility that the observed transient substrate of SCD is sex-specific. Further studies of SCD triggers in women are needed. While we performed robust internal validation of our findings using bootstrapping in five partitions of the dataset, replication of the SCD trigger analyses in another prospective cohort is needed. Nevertheless, this is the largest prospective study of SCD triggers and substrates, suggesting differences between long-term and transient SCD-specific and non-SCD-specific substrates [36]. In this study, correlation between GEH metrics and heart rate was weak (r values between 0.1–0.2), and we did not normalize GEH metrics by heart rate. However, further studies are needed to determine whether normalization by heart rate can further improve the predictive value of GEH.

Conclusions

Dynamic predictive accuracy of ECG and VCG biomarkers should be taken into account for the development of dynamic risk scores of competing SCD risk. The distinction between markers predicting short-term and long-term events may represent the difference between markers heralding SCD (triggers or transient substrates) versus markers identifying persistent substrate.

Supplementary information

Supplementary information accompanies this paper at <https://doi.org/10.1186/s12872-019-1234-9>.

Additional file 1: Table S1. Time-dependent AUC with 95% Confidence Interval for prediction of SCD and non-SCD, for windows of prediction 3, 6, 9 months, 1, 2, 3, 5, 10, 15 years for traditional ECG markers, and GEH-ECG in five partitions of the study dataset. See separate excel file. $_lb$ = lower bound; $_ub$ = upper bound. HR = heart rate; qtc = QTc interval; qrs = QRS interval; pQRST = peak QRS-T angle; aQRST = area QRS-T angle; pSVGaz = peak SVG azimuth; aSVGaz = area SVG azimuth; pSVGel = peak SVG elevation; aSVGel = area SVG elevation; pSVGmag = peak SVG magnitude; aSVGmag = area SVG magnitude. SAI = Sum Absolute QRST Integral (SAI QRST).

Abbreviations

AF: Atrial fibrillation; ARIC: Atherosclerosis risk in community study; AUC: Area under the curve; AV: Atrioventricular; CHD: Coronary heart disease; CI: Confidence interval; CVD: Cardiovascular disease; ECG: Electrocardiogram; GEH: Global electrical heterogeneity; HF: Heart failure; IDI: Integrated discrimination improvement; LV: Left ventricle; MI: Myocardial infarction; Non-SCD: Non-sudden cardiac death; NRI: Net reclassification improvement; PAD: Peripheral artery disease; ROC: Receiver operating characteristic; RVOT: Right ventricular outflow tract; SAI QRST: Sum absolute QRST integral; SCD: Sudden cardiac death; SD: Standard deviation; SVG: Spatial ventricular gradient; US: United States; VM: Vector magnitude

Acknowledgements

The authors thank the staff and participants of the ARIC study for their important contributions. We would like to acknowledge the SCD mortality classification committee members: Nona Sotoodehnia (lead), Selcuk Adabag, Sunil Agarwal, Lin Chen, Rajat Deo, Leonard Ilkhanoff, Liviu Klein, Saman Nazarian, Ashleigh Owen, Kris Patton, and Larisa Tereshchenko.

Authors' contributions

EAPA and LGT designed the study. AB, DG, SVM and LGT reviewed 12-lead ECGs and adjudicated origin and conduction of each cardiac beat. EAPA and YLP developed MATLAB software code for automated ECG analyses and analyzed digital ECG signal. CH and JT checked quality of automated ECG analysis and verified accuracy of fiducial points detection. LGT performed the statistical analyses. EAPA and LGT wrote the first draft of the manuscript. All authors participated in data interpretation, discussion and preparation of the final manuscript, and read and approved the final manuscript.

Funding

The ARIC study has been funded in whole or in part with Federal funds from the National Heart, Lung, and Blood Institute, National Institutes of Health, Department of Health and Human Services, under Contract nos. (HHSN268201700001), HHSN268201700002), HHSN268201700003), HHSN268201700004), HHSN268201700005). This work was supported by HL118277 (LGT). The funding body had no role in the design of the study and collection, analysis, and interpretation of data and in writing the manuscript.

Availability of data and materials

After the ethical approval at a requestor institution, the de-identified ARIC data can be obtained from the National Heart, Lung, and Blood Institute – maintained BioLINCC repository [37], and via ARIC Coordinating Center at the University of North Carolina—Chapel Hill [38]. The BioLINCC website [37] includes detailed information about the process to obtain such data. Details about the procedures for data request from the ARIC Coordinating Center at the University of North Carolina—Chapel Hill can be found online [38]. GEH results were reported to the ARIC Coordinating Center by the ARIC ancillary study “Novel ECG measures and risk of sudden cardiac death” (principal investigator Tereshchenko). We provided open-source MATLAB (MathWorks, Natick, MA, USA) code at: <https://github.com/Tereshchenkolab/Global-Electrical-Heterogeneity>, and <https://github.com/Tereshchenkolab/Origin>. SCD risk calculator is available at <http://www.ecgpredictscd.org>.

Ethics approval and consent to participate

This study was approved by the Oregon Health & Science University and the Johns Hopkins University Institutional Review boards (IRB). The ARIC study protocol was approved by the IRB at all participating institutions: University of North Carolina at Chapel Hill IRB, Johns Hopkins University IRB, University of Mississippi Medical Center IRB, and University of Minnesota IRB. All participants signed informed consent before entering the study. The study protocol conforms to the ethical guidelines of the 1975 Declaration of Helsinki.

Consent for publication

Not applicable.

Competing interests

The authors declare that they have no competing interests.

Author details

¹Knight Cardiovascular Institute, Department of Medicine, Oregon Health & Science University School of Medicine, 3181 SW Sam Jackson Park Rd; UHN62, Portland, OR 97239, USA. ²Department of Biomedical Informatics, Emory University, Atlanta, GA, USA. ³UCLA Cardiac Arrhythmia Center, University of California Los Angeles, Los Angeles, CA, USA. ⁴Rush University, Chicago, IL, USA. ⁵Rosalind Franklin University of Medicine and Science, North Chicago, IL, USA. ⁶University of Washington, Seattle, WA, USA. ⁷Cardiovascular Division, Department of Medicine, Johns Hopkins University School of Medicine, Baltimore, MD, USA.

Received: 7 June 2019 Accepted: 23 October 2019

Published online: 14 November 2019

References

- Benjamin EJ, Virani SS, Callaway CW, Chamberlain AM, Chang AR, Cheng S, et al. Heart disease and stroke Statistics-2018 update: a report from the American Heart Association. *Circulation*. 2018;137(12):e67–e492.
- Stecker EC, Reinier K, Marijon E, Narayanan K, Teodorescu C, Uy-Evanado A, et al. Public health burden of sudden cardiac death in the United States. *Circ Arrhythm Electrophysiol*. 2014;7(2):212–7.
- Morin DP, Link MS. Advances in the risk stratification, prevention, and treatment of sudden cardiac death. *Prog Cardiovasc Dis*. 2019;62(3):203–4.
- Waks JW, Sitlani CM, Soliman EZ, Kabir M, Ghafoori E, Biggs ML, et al. Global electrical heterogeneity risk score for prediction of sudden cardiac death in the general population: the atherosclerosis risk in communities (ARIC) and cardiovascular health (CHS) studies. *Circulation*. 2016;133(23):2222–34.
- Tereshchenko LG, Sotoodehnia N, Sitlani CM, Ashar FN, Kabir M, Biggs ML, et al. Genome-wide associations of global electrical heterogeneity ECG phenotype: the ARIC (atherosclerosis risk in communities) study and CHS (cardiovascular health study). *J Am Heart Assoc*. 2018;7(8):e008160.
- The ARIC Investigators. The atherosclerosis risk in community (ARIC) study: design and objectives. *Am J Epidemiol*. 1989;129(4):687–702.
- Blackburn H, Keys A, Simonson E, Rautaharju P, Punsar S. The electrocardiogram in population studies. A classification system. *Circulation*. 1960;21:1160–75.
- Eriksson H, Caidahl K, Larsson B, Ohlson LO, Welin L, Wilhelmsen L, et al. Cardiac and pulmonary causes of dyspnoea—validation of a scoring test for clinical-epidemiological use: the study of men born in 1913. *Eur Heart J*. 1987;8(9):1007–14.
- Toole JF, Chambless LE, Heiss G, Tyroler HA, Paton CC. Prevalence of stroke and transient ischemic attacks in the atherosclerosis risk in communities (ARIC) study. *Ann Epidemiol*. 1993;3(5):500–3.
- Weatherley BD, Chambless LE, Heiss G, Catellier DJ, Ellison CR. The reliability of the ankle-brachial index in the atherosclerosis risk in communities (ARIC) study and the NHLBI family heart study (FHS). *BMC Cardiovasc Disord*. 2006;6:7.
- White AD, Folsom AR, Chambless LE, Sharret AR, Yang K, Conwill D, et al. Community surveillance of coronary heart disease in the atherosclerosis risk in communities (ARIC) study: methods and initial two years' experience. *J Clin Epidemiol*. 1996;49(2):223–33.
- Bogle BM, Sotoodehnia N, Kucharska-Newton AM, Rosamond WD. Vital exhaustion and sudden cardiac death in the atherosclerosis risk in communities study. *Heart*. 2018;104(5):423–9.
- Thomas JA, AP-A E, Junell A, Newton K, Hamilton C, Li-Pershing Y, et al. Vectorcardiogram in athletes: The Sun Valley Ski Study. *Ann Noninvasive Electrocardiol*. 2019;24(3):e12614.
- Perez-Alday EA, Li-Pershing Y, Bender A, Hamilton C, Thomas JA, Johnson K, et al. Importance of the heart vector origin point definition for an ECG analysis: the atherosclerosis risk in communities (ARIC) study. *Comput Biol Med*. 2019;104:127–38.
- Sur S, Han L, Tereshchenko LG. Comparison of sum absolute QRST integral, and temporal variability in depolarization and repolarization, measured by dynamic vectorcardiography approach, in healthy men and women. *PLoS One*. 2013;8(2):e57175.
- Kors JA, van HG SAC, van Bommel JH. Reconstruction of the frank vectorcardiogram from standard electrocardiographic leads: diagnostic comparison of different methods. *Eur Heart J*. 1990;11(12):1083–92.
- Heagerty PJ, Lumley T, Pepe MS. Time-dependent ROC curves for censored survival data and a diagnostic marker. *Biometrics*. 2000;56(2):337–44.
- Cattaneo M, Malighetti P, Spinelli D. Estimating receiver operative characteristic curves for time-dependent outcomes: the stroccurve package. *Stata J*. 2017;17(4):1015–23.
- Pencina MJ, D'Agostino RB Sr, D'Agostino RB Jr, Vasan RS. Evaluating the added predictive ability of a new marker: from area under the ROC curve to reclassification and beyond. *Stat Med*. 2008;27(2):157–72 discussion 207–12.
- Pencina MJ, D'Agostino RB Sr, Steyerberg EW. Extensions of net reclassification improvement calculations to measure usefulness of new biomarkers. *StatMed*. 2011;30(1):11–21.
- Zipes DP, Wellens HJ. Sudden cardiac death. *Circulation*. 1998;98(21):2334–51.
- Waks JW, Tereshchenko LG. Global electrical heterogeneity: a review of the spatial ventricular gradient. *J Electrocardiol*. 2016;49(6):824–30.
- Noda T, Shimizu W, Taguchi A, Aiba T, Satomi K, Suyama K, et al. Malignant entity of idiopathic ventricular fibrillation and polymorphic ventricular tachycardia initiated by premature extrasystoles originating from the right ventricular outflow tract. *J Am Coll Cardiol*. 2005;46(7):1288–94.
- Boukens BJ, Christoffels VM, Coronel R, Moorman AF. Developmental basis for electrophysiological heterogeneity in the ventricular and outflow tract myocardium as a substrate for life-threatening ventricular arrhythmias. *Circ Res*. 2009;104(1):19–31.
- Ashar FN, Mitchell RN, Albert CM, Newton-Cheh C, Brody JA, Muller-Nurasyid M, et al. A comprehensive evaluation of the genetic architecture of sudden cardiac arrest. *Eur Heart J*. 2018;39(44):3961–9.
- Wilson FN, Macleod AG, Barker PS, Johnston FD. The determination and the significance of the areas of the ventricular deflections of the electrocardiogram. *Am Heart J*. 1934;10(1):46–61.
- Burger HC. A theoretical elucidation of the notion ventricular gradient. *Am Heart J*. 1957;53(2):240–6.
- Oehler A, Feldman T, Henrikson CA, Tereshchenko LG. QRS-T angle: a review. *Annals Noninvasive Electrocardiol*. 2014;19(6):534–42.
- Tereshchenko LG, McNitt S, Han L, Berger RD, Zareba W. ECG marker of adverse electrical remodeling post-myocardial infarction predicts outcomes in MADIT II study. *PLoS One*. 2012;7(12):e51812.
- Tereshchenko LG, Cheng AA, Fetis BJ, Butcher B, Marine JE, Spragg DD, et al. A new electrocardiogram marker to identify patients at low risk for ventricular tachyarrhythmias: sum magnitude of the absolute QRST integral. *J Electrocardiol*. 2011;44(2):208–16.
- Kozmann G, Tuboly G, Szathmáry V, Švehlíková J, Tyšler M. Computer modelling of beat-to-beat repolarization heterogeneity in human cardiac ventricles. *Biom Signal Process Control*. 2014;14(0):285–90.
- Tereshchenko LG, Cheng A, Fetis BJ, Marine JE, Spragg DD, Sinha S, et al. Ventricular arrhythmia is predicted by sum absolute QRST integral but not by QRS width. *J Electrocardiol*. 2010;43(6):548–52.
- Perez-Alday E, Hamilton CL-P, Monroy-Trujillo Y, Estrella JM, Sozio M, Jaar S, Parekh B, Rulan Tereshchenko L. The Reproducibility of Global Electrical Heterogeneity ECG Measurements. *Computing in cardiology: IEEE Explore*; 2018. p. 162–6.
- Deo R, Norby FL, Katz R, Sotoodehnia N, Adabag S, DeFilippi CR, et al. Development and validation of a sudden cardiac death prediction model for the general population. *Circulation*. 2016;134(11):806–16.
- Bogle BM, Ning H, Goldberger JJ, Mehrotra S, Lloyd-Jones DM. A simple community-based risk-prediction score for sudden cardiac death. *Am J Med*. 2018;131(5):532–9 e5.

36. Escobar-Robledo LA, Bayes-de-Luna A, Lupon J, Baranchuk A, Moliner P, Martinez-Selles M, et al. Advanced interatrial block predicts new-onset atrial fibrillation and ischemic stroke in patients with heart failure: the "Bayes' syndrome-HF" study. *Int J Cardiol.* 2018;271:174–80.
37. NIH/NHLBI. Biologic Specimen and Data Repository Information Coordinating Center. 1987. Available at: <https://biolincc.nhlbi.nih.gov/>. Accessed 22 June 2018.
38. ARIC. Study Description. 1987. Available at: <http://www2.csc.unc.edu/aric/distribution-agreements>. Accessed June 22nd, 2018. <http://www2.csc.unc.edu/aric/distribution-agreements>

Publisher's Note

Springer Nature remains neutral with regard to jurisdictional claims in published maps and institutional affiliations.

Ready to submit your research? Choose BMC and benefit from:

- fast, convenient online submission
- thorough peer review by experienced researchers in your field
- rapid publication on acceptance
- support for research data, including large and complex data types
- gold Open Access which fosters wider collaboration and increased citations
- maximum visibility for your research: over 100M website views per year

At BMC, research is always in progress.

Learn more biomedcentral.com/submissions

